Computational Model of Spinal Hemiepiphysiodesis

Effects of Implant-Bone Contact, Initial Disc Wedging, and Growth

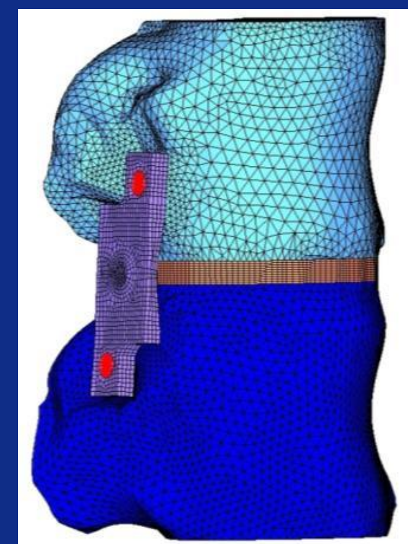

Kumar B, Bylski-Austrow DI, Wall EJ, Liu YJ

Background and Significance

- A titanium implant construct for spine growth modification has been FDA approved for early stage clinical trial for AIS
- Early design showed staple construct (SS) caused curvatures in normal spines within 2 months [1]
  - Growth plate histomorphometry indicated compression gradient [2]
- Disc wedging from intervertebral rotation due to implant insertion determined in vitro [3]

Immediate post-op 2 months

Previous studies

- Finite element model (FEM) developed with biomechanical tests
  - Continuum model of annulus [4]
- FEM and tests correlated well for control motion segment (no implant)
  - Compared to compression tests
- Addition of implant to FEM overestimated stiffness
  - FEM assumptions
    - Perfect bone-implant contact
    - No changes in orientation or disc stress due to implantation
- Quantitative relationship between growth and compressive stress
  - Stokes et al [5,6]

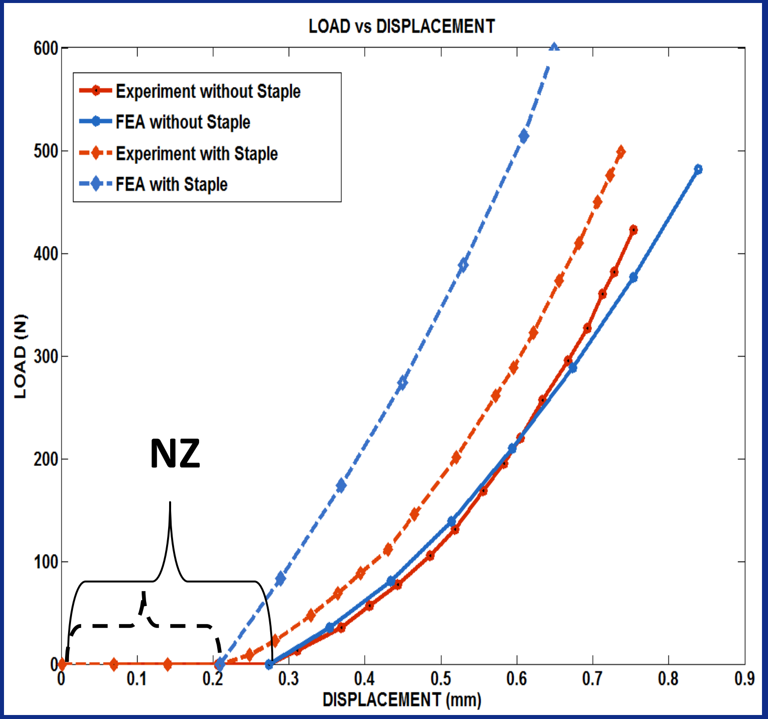

Purpose

- **Determine whether**

  1. **Changes to selected FEM parameters improves correlation with tests**
     - **Contact between implant and bone**
     - **Initial biomechanical gradients**
       - **Disc wedging due to implant insertion**

  2. **Addition of a growth-stress relationship produces asymmetric growth patterns**
     - **Compared to experimental histomorphometric results**

Methods – FEM Construction

- **3-D FEM from CT scan of T7-T8 porcine spine**
  - **Cortical, cancellous, end plates [7]**
  - **Annulus fibrosus modeled using anisotropic hyperelastic material properties [4]**
  - **Interface properties between bone-implant**
    - **Coefficient of friction varied from 0.1 – 0.3**
    - **Soft normal interaction property [8]**
  - **Initial conditions due to implantation**
    - **2 degree coronal plane tilt**
      - **Neutral axis central**
    - **With and without residual disc stress**

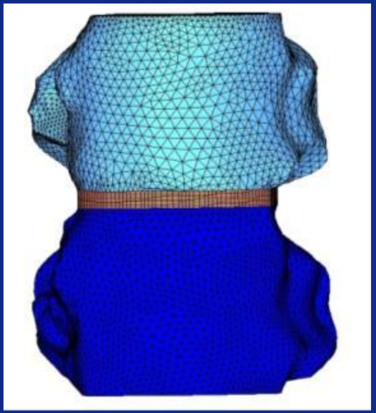

Coronal view, FEM, porcine spinal segment without implant

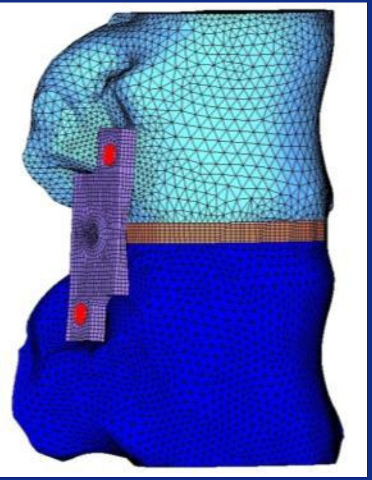

Oblique view, FEM with implant

Methods

- **FEM created in Hypermesh**
- **Compression test simulated**
  - **Boundary conditions**
    - **Caudad nodes constrained in longitudinal axial direction**
      - **Few additional nodes constrained to avoid rigid body modes**
  - **Loads**
    - **Axial displacements applied**

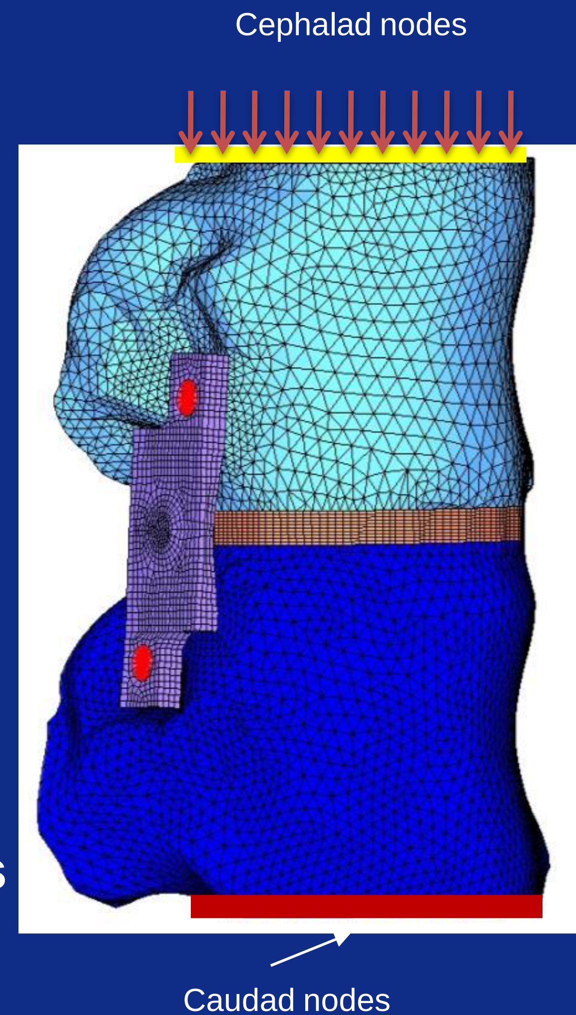

Solving

- **FEM imported to Abaqus (v6.8-2)**
- **Nonlinear large deformation static analyses**
  - **Material and geometric nonlinearities**

Methods – Growth Model

- Linear growth model added [5,6,9]
  - $\beta = 1.2\ \text{MPa}^{-1}$

$$\varepsilon_m = \delta G_y + \beta_y \delta\sigma_y \delta G_y$$

- Growth plates added to FEM
- Initial baseline growth applied
  - In terms of temperature strain
- Growth modulation strains calculated
  - Applied static compressive stress of 0.5 MPa
- Iterations simulated 2 month post-op time

Growth plates

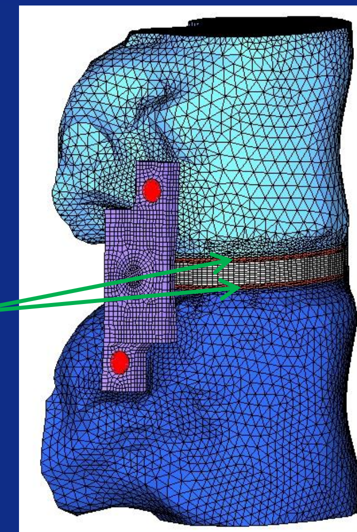

Oblique view, FEM, spinal segment including growth regions and implant

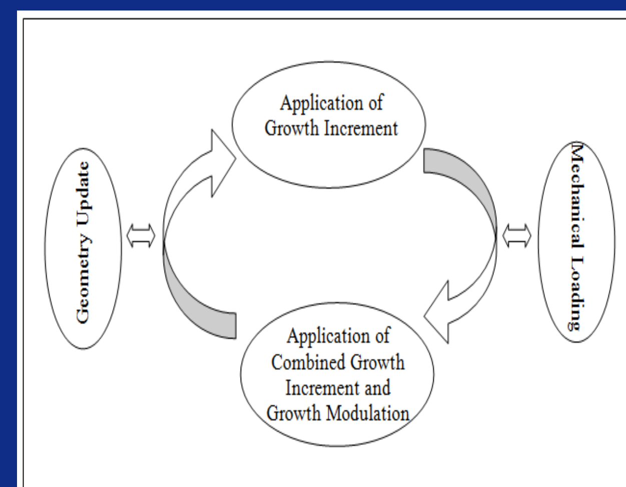

Sequential procedures for strain/growth increments

Results – Load vs Displacement Curves

- To compare L-d curves from FEM to biomechanical tests
  - Neutral zone (NZ) added
- FEM with either friction or soft normal contact
  - Less stiff than perfect contact
  - Stiffer than experiments
- Frictional contact
  - Linear response
- Soft contact
  - Nonlinear behavior
  - Better simulation of experiments

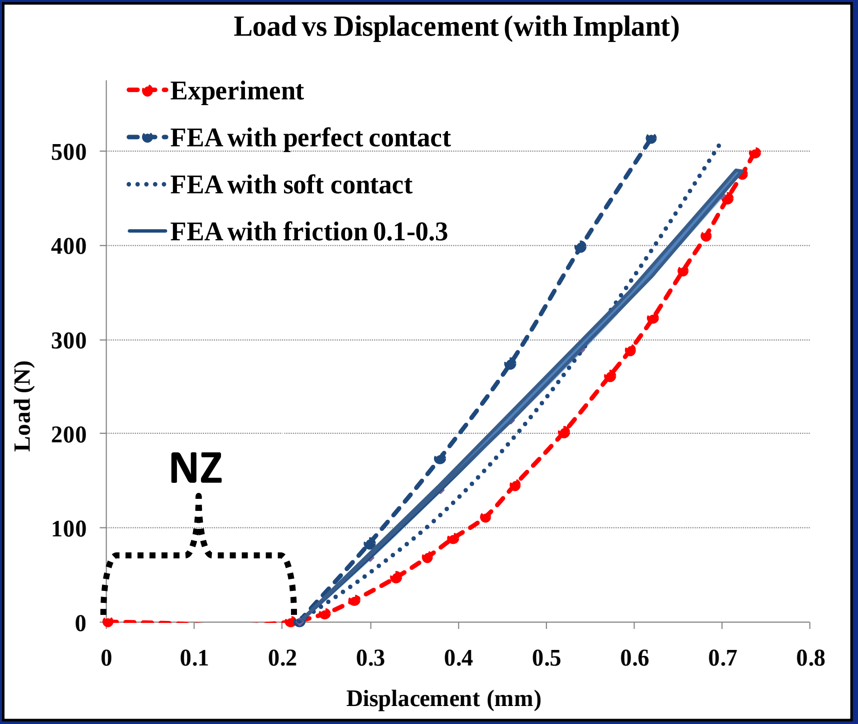

Compressive load - displacement behavior

Results – Initial Conditions

- **Disc wedging of 2 degrees**
  - ***Without* residual disc compressive stresses**
    - **Did not affect stiffness**
  - ***With* residual disc stresses**
    - **Increased stiffness compared to both experiment and FEM with perfect contact conditions**

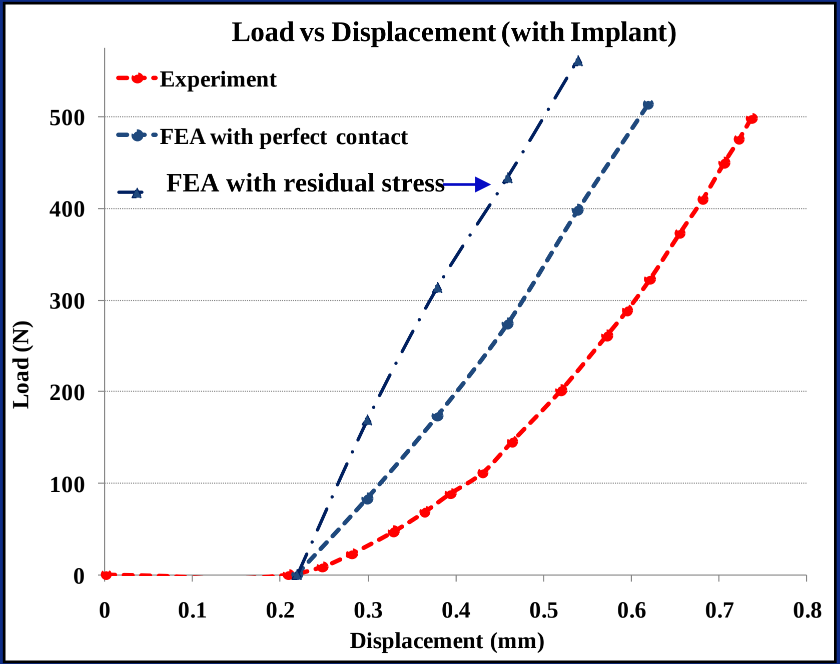

Load displacement curves from FEM with different initial conditions

Results – Growth

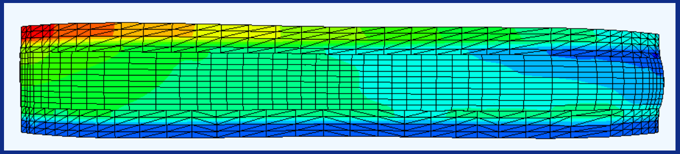

Growth plot after two iterations, post-op 2 months, showing maximum growth on contralateral side

- **Asymmetric growth at 2 months**
  - **Growth reduced across coronal plane**

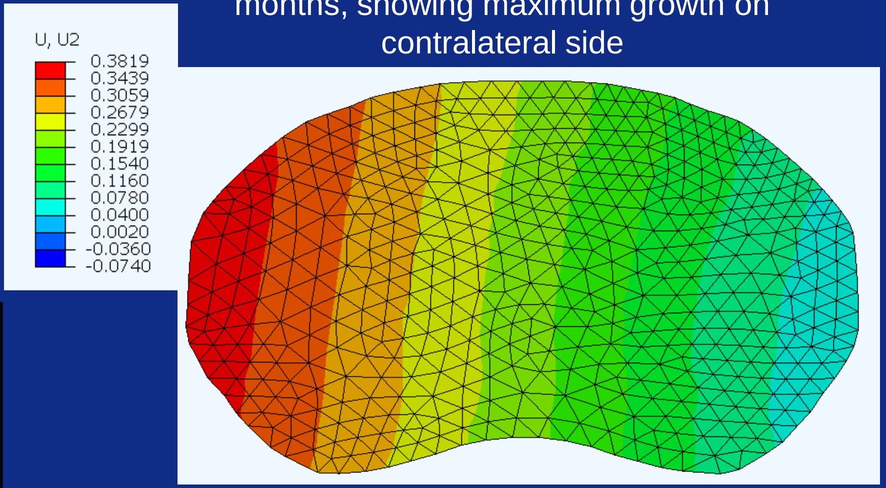

Growth distribution across cephalad growth plate at end of two iterations

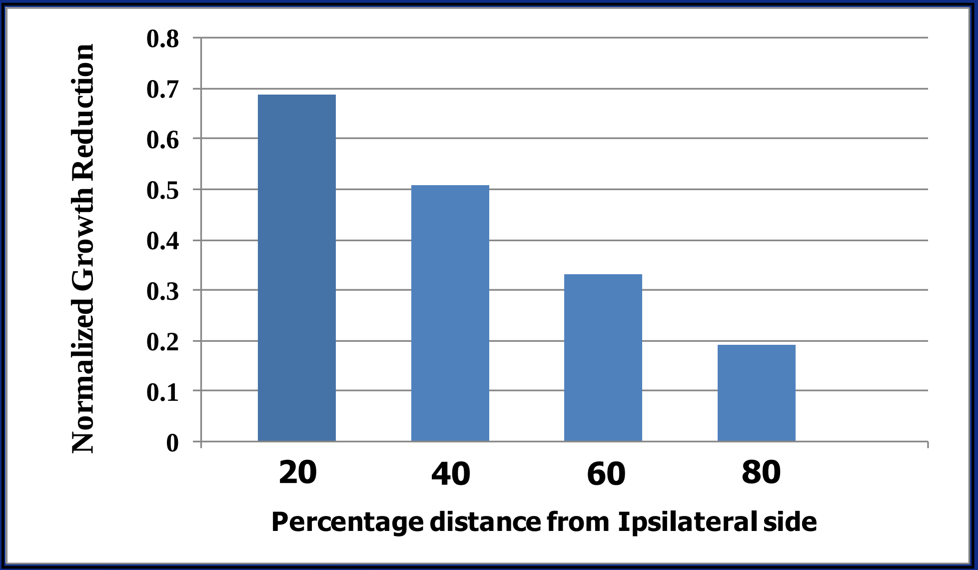

- **Reduction in growth**
  - **Ipsilateral side reduced by 69%**
  - **Contralateral side by 20%**

Conclusions / Discussion

- FEA used for parametric analyses and growth simulations
  - Within one type of implant
  - With consideration of in vitro and in vivo tests
- Bone-implant interfaces
  - Soft and friction both better simulated tests compared to perfect contact
- Initial conditions
  - Disc wedging did not improve agreement with in vitro tests
    - Regardless of residual disc stresses
- Growth modification
  - Asymmetric inhibition across coronal plane
  - Similar to pattern reported for growth plate histomorphometry [2]
    - Greater reductions in growth predicted especially on ipsilateral side

Limitations

- Current model: Rotational and combined loading validations required
- FEM in general
  - Inability to model neutral zone (rigid body motion)
  - Large numbers of parameters affect results, careful application required

References

1. Wall EJ, Bylski-Austrow DI, Kolata RJ, Crawford AH (2005) Endoscopic mechanical spinal hemiepiphysiodesis modifies spine growth. Spine 30, 1148–1153
2. Bylski-Austrow DI, Wall EJ, Glos DL, Ballard ET, Montgomery A, Crawford AH (2009) Spinal hemiepiphysiodesis decreases the size of vertebral growth plate hypertrophic zone and cells. J Bone Joint Surg Am 91, 584-593
3. Bylski-Austrow DI, Glos DL, Boehm LA, Jain VV, Wall EJ. Coronal plane displacement gradient precedes vertebral growth modification using titanium spinal hemiepiphyseal staples (2010) ICEOS #17
4. Eberlein R, Holzapfel GA, Schulze-Bauer CAJ (2001) An anisotropic model for annulus tissue and enhanced finite element analyses of intact lumbar disc bodies. Computer Methods in Biomechanics and Biomedical Engineering 4: 209 -229
5. Stokes IAF, Laible J. (1990) Three-dimensional osseo-ligamentous model of the thorax representing initiation of scoliosis by asymmetric growth. J Biomech 23:589-595.
6. Stokes IAF (2007) Analysis and simulation of progressive adolescent scoliosis by biomechanical growth modulation. Eur Spine J. 16:1621-1628
7. Kumar B, Bylski-Austrow DI, Wall EJ, Liu YJ (2010) Finite element analysis of compressive properties and disc stresses before and after spinal hemiepiphysiodesis", 4th ICEOS, #113
8. Ihlde S, Goldmann T, Himmlova L, Aleksic Z. (2008) The use of finite element analysis to model bone-implant contact with basal implants. Oral Surgery, Oral Medicine, Oral Pathology, Oral Radiology, and Endodontology (OOOOE) 106:39-48.
9. Villemure I, Aubin CE, Dansereau J, Labelle H. (2002) Simulation of progressive deformities in adolescent idiopathic scoliosis using a biomechanical model integrating vertebral growth modulation. J Biomech Eng 124:784-790

Acknowledgment

University Orthopaedic Research and Education Foundation